Iterative Edge- and Wavelet-Based Image Registration of AVHRR and GOES Satellite Imagery

Jacqueline Le Moigne [1] *, Nazmi El-Saleous* [2]*, Eric Vermote* [2]
lemoigne@cesdis.gsfc.nasa.gov

(1) USRA/CESDIS; (2) University of Maryland
Contact: Code 930.5, Goddard Space Flight Center, Greenbelt, MD 20771

Abstract

Most automatic registration methods are either correlation-based, feature-based, or a combination of both. Examples of features which can be utilized for automatic image registration are edges, regions, corners, or wavelet-extracted features. In this paper, we describe two proposed approaches, based on edge or edge-like features, which are very appropriate to highlight regions of interest such as coastlines. The two iterative methods utilize the Normalized Cross-Correlation of edge and wavelet features and are applied to such problems as image-to-map registration, landmarking, and channel-to-channel co-registration, utilizing test data, AVHRR data, as well as GOES image data.

1. Introduction

Digital image registration is very important in many applications of image processing, such as medical imagery, robotics, visual inspection, and remotely sensed data processing. For all of these applications, image registration is defined as the process which determines the most accurate match between two or more images acquired at the same or at different times by different or identical sensors. Registration provides the "relative" orientation of two images (or one image and other sources, e.g., a map), with respect to each other, from which the absolute orientation into an absolute reference system can be derived. Image registration is usually motivated by such goals as object recognition, model matching, pose estimation, or change detection. In this paper, we will only refer to remote sensing applications, for which automated image geo-registration has become a highly desirable technique.

Currently, the most common approach to remotely sensed image registration is to extract a few outstanding characteristics of the data, which are called *control points* (CP's), *tie-points,* or *reference points*. The CP's (usually selected interactively) in both images (or image and map) are matched by pair and used to compute the parameters of a geometric transformation. But such a point selection represents a repetitive, labor- and time-intensive task which becomes prohibitive for large amounts of data. Also, too few points, inaccurate points, or ill-distributed points might be chosen thus leading to large registration errors. Recently, a relatively important number of automatic image registration methods have been developed [1,2], and they focus on the automatic selection of the control points, on the speed of processing as well as on the accuracy of the resulting registration. Most automatic registration methods are either correlation-based, feature-based, or a combination of both. Examples of features which are utilized for registration are edges, regions, corners, or wavelet-extracted features

In this paper, we describe two proposed approaches based on edge or edge-like features, which are very appropriate to highlight regions of interest such as coastlines. These two algorithms perform automatic image registration in an iterative manner, first estimating the parameters of the transformation, and then iteratively refining these parameters. Preliminary results are presented utilizing test data, as well as map-to-image registration of AVHRR image data, and landmarking and co-registration of GOES data.

2. Edge- and Wavelet-Based Registrations

Among all potential features to utilize as control points, edges and edge-like features appear as ones of the most promising. Often, a human operator will choose sharp curvatures in coastlines or rivers, the intersections of two roads or the coastline of a lake as control points to perform manual registration. The initial approaches presented in this paper are based on these observations as well as on the conclusions of three previous studies [3,4,5] which compare manual registration, edge matching, and phase correlation. All these converge to conclude that edge or edge-like features are very appropriate to highlight regions of interest such as coastlines. In one of these studies [4], the Normalized Cross-Correlation [6] is rated as one of the best matching measures. Therefore, in this study we present the results obtained by two methods based on the Normalized Cross-Correlation of edge and wavelet features.

2.1 Edge Detection

An edge detection computes the gradient of the original gray levels and highlights the pixels of the image with higher contrast. Since edge values are less affected by local intensity variations or time-of-the day conditions than original gray level values, edge features should be more reliable than original gray levels. Figure 1 shows on an example of a coastline how edge detection can be useful to detect the exact location of the edge point A located on the coastline: if we draw a line perpendicular to the coastline at point A, and we consider the function representing the intensity of the image points along this line, we get a function which is about constant over the land, jumps down at the edge and gets constant again over the water. If we compute the gradient (or first derivative) of this function, we get a edge function which is about zero everywhere except around the edge point where it reaches a maximum. Locating this maximum is equivalent to finding the edge point, i.e. the coastline point A in this example.

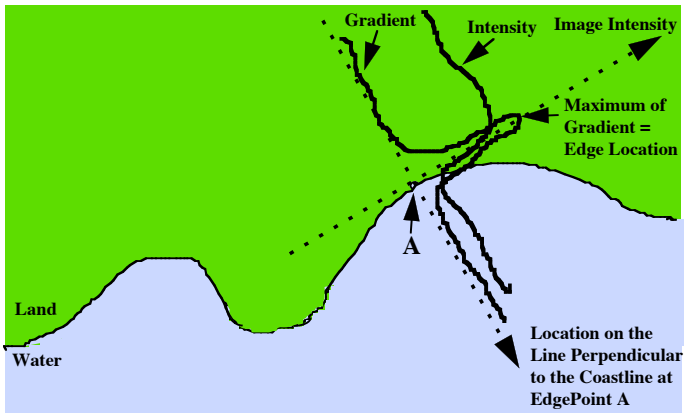

Figure 1
Edge Detection for Coastlines Extraction

In the method presented below, we will be using a Sobel edge detector which computes the gradient (or first derivative) of the 2-D image signal through two filters, an horizontal filter, Fh and a vertical filter, Fv:

$$Fv = \begin{bmatrix} -1 & -2 & -1 \\ 0 & 0 & 0 \\ 1 & 2 & 1 \end{bmatrix} \qquad Fh = \begin{bmatrix} -1 & 0 & 1 \\ -2 & 0 & 2 \\ -1 & 0 & 1 \end{bmatrix}$$

The magnitude of the gradient is computed as:

$M = \mathrm{Sqrt}(Fv^2 + Fh^2)$

and the direction at each point is computed as:

$D = \mathrm{Arctg}(Fv/Fh)$.

Higher magnitudes values of M correspond to edge features including coastlines. Other edge detection methods [7,8], computationally more expensive but less sensitive to noise, will be investigated later.

2.2. Wavelet Decomposition

Similarly to a Fourier transform, wavelet transforms provide a time-frequency representation of a signal, which can be inverted for later reconstruction. However, the wavelet representation allows a better spatial localization as well as a better division of the time-frequency plane than a Fourier transform, or than a windowed Fourier transform. In a wavelet representation, the original signal is filtered by the translations and the dilations of a basic function, called the "mother wavelet". For the algorithm described below, only discrete orthonormal basis of wavelets have been considered and have been implemented by filtering the original image by a high-pass and a low-pass filter, thus in a multi-resolution fashion. At each level of decomposition, four new images are computed; each of these images is half the size of the previous original image and represents the low frequency or high frequency information of the image in the horizontal or/and the vertical directions; images LL (Low/Low), LH (Low/High), HL(High/Low), and HH (High/High) of Table 1. Starting again from the "compressed" image (or image representing the low-frequency information), the process can be iterated, thus building a hierarchy of lower and lower resolution images. Table 1 summarizes the multi-resolution decomposition.

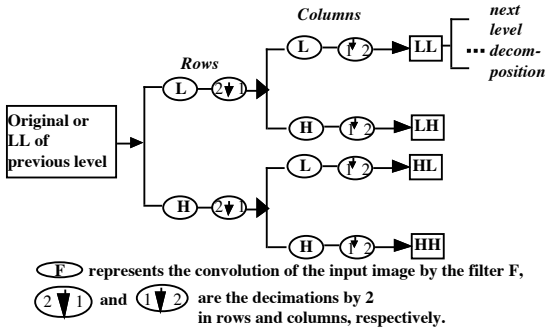

Table 1
Multi-Resolution Wavelet Decomposition

The features provided through this type of wavelet decomposition are of two different types: the low-pass features which provide a compressed version of the original data and some texture information, and the high-pass features which provide detailed information very similar to edge features. The advantages of using a wavelet decomposition are twofold; (a) by considering the low-pass information, one can bring different spatial resolution data to a common spatial resolution without losing any significant features, which is very useful for channel-to-channel co-registration or registration of multi-resolution data, (b) by utilizing high-pass information, one can retrieve significant features which are correlated in the registration process, similarly to edge features. When these features are extracted at a lower resolution, only the strongest features are still present, thus eliminating weak higher resolution features. Furthermore, utilizing wavelet transforms ties wavelet-based registration algorithms to a more general data management framework [9], in which wavelet

decomposition could serve the multi-purpose of image compression, reconstruction, and content extraction as well as image registration.

Our wavelet-based registration algorithm [2,10,11] is based on the high-frequency information extracted from the wavelet decomposition (images "LH" and "HL" from Table 1). Only those points whose intensities belong to the top *x*% of the histograms of these images are kept (*x* being a parameter of the program whose selection can be automatic); we call these points "maxima of the wavelet coefficients," and these maxima form the feature space.

2.3 Feature Matching

Correlation measurement is the usual similarity metric [6], although it is computationally expensive and noise sensitive when used on original gray level data. Using a pre-processing such as edge detection or a wavelet multi-resolution search strategy enables large reductions in computing time and increases the robustness of the algorithms. If R and I are the reference and the input images, the correlation measure between R and I is defined by:

$$\mathrm{Corr}(R,I) = \frac{\Sigma((Rj-R^*).(Ij-I^*))}{\sqrt{\Sigma(Rj-R^*)^2 \,.\, \Sigma(Ij-I^*)^2}}$$

with R^* and I^* are the mean of images R and I, respectively. Other similarity metrics are described in [12] and will be evaluated in future work as well as the use of a robust feature matching algorithm which is described in [13].

2.4 Description of the Two Algorithms

In general, we will assume the transformation to be either a rigid or an affine transformation. Although high-order polynomials are superior to isometric transformations when the deformation includes more than a translation and a rotation, isometric transformations are more accurate when a smaller number of points is available and are less sensitive to noise and to largely inconsistent tie-points. Both types of transformations include compositions of translations and rotations; therefore, as a preliminary study, our search space is composed of rigid transformations for the edge-based method and compositions of 2-D rotations and translations for the wavelet-based method, and will be extended later to affine transformations. Both edge- and wavelet-based methods represent a three-step approach to automatic registration of remote sensing imagery. The first step involves the edge extraction or the wavelet decomposition of the reference and input images to be registered. In the second step, we extract domain independent features from both reference and input images. In the wavelet method, feature extraction is performed at each decomposition level. Finally, we utilize these features to compute the transformation function. Both methods perform the registration in an iterative manner, first estimating the parameters of the deformation transformation, and then iteratively refining these parameters.

For the edge-based implementation, we chose to model the transformation as a combination of a scaling in both directions (dsx,dsy), a rotation (dΘ), and a shift or translation (dtx,dty)in both directions. This algorithm is based on the assumption that rotation angle and scaling parameters are small (within 5 degrees for the rotation angle and within [0.9,1.1] for the scaling parameters). At the first iteration, the translation parameters are first extracted assuming rotation and scaling to be negligible. Then, knowing the translation parameters, the rotation angle is found, assuming the scaling negligible. Then scaling parameters are retrieved. At each next iteration, the five parameters are retrieved simultaneously, by computing the cross-correlations for all successive values of the parameters taken at incremental steps. At each iteration, the accuracy on the transformation parameters is divided by two. So, if at the first iteration, the translation parameters are found at a 1 pixel accuracy, the accuracy will be 0.5 pixel at iteration 2, 0.25 at iteration 3, etc.

For the wavelet-based method, the search intervals on the parameters can either be chosen arbitrarily or be reduced by the user utilizing a priori information about the sensor movement and the satellite navigation system. The search strategy is explained below when looking only for rotations and follows the multiresolution provided by the wavelet decomposition. At the deepest level of decomposition (where the image size is the smallest), the search is exhaustive over the whole search space (e.g., [0,90degrees]) but with an accuracy equal to Δ (e.g., 8 degrees). The first approximation of the best rotation, Rn, is chosen over this search space; then Rn becomes the center of a new search interval of length 2Δ, [Rn - Δ , Rn + Δ], and at the next lower level, the new approximated rotation, Rn-1, is found within this search interval with an accuracy of Δ/2. This process is repeated until the first level of decomposition, where the search interval is [R2 - Δ/2**(n-2), R2 + Δ/2**(n-2)] and the final registration rotation, R1, is found with an accuracy equal to Δ/2**(n-1). In particular, if δ is the desired registration accuracy (e.g., 1 degree), Δ is chosen as 2**(n-1) δ, where n is the number of levels of wavelet decomposition. In the case of an affine transformation, instead of looking for all parameters simultaneously, the search is performed over each set of parameters independently, first looking for shifts, then for rotations, etc. Such a use of successive "subsearches" reduces dramatically the amount of computations. Other solutions will be investigated, such as the use of an optimization technique or of a statistically robust point matching method [13].

Below is a more general description of both registration algorithms using edge or wavelet features for AVHRR and GOES image data:

(R1) *Preprocessing Step:* The pre-processing step enhances the contrast of the features which are utilized to perform the registration. For some channels, gray levels may have to be inverted to consider homogeneous computations.

(R2) *Wavelet Decomposition:* Since images to be registered may have different spatial resolutions, the wavelet decomposition step brings these images to a common spatial resolution without degrading the image quality. Wavelet decomposition is pursued further down if wavelet coefficients are used for the registration.

(R3) *Registration:* This step can be performed by cross-correlating either edge features or wavelet features. With either type of features, the registration is performed by:

(R3.1) Estimating independently the five parameters: rotation, shift in the x-direction, shift in the y-direction, scaling in x, and scaling in y. First the rotation and the scalings are assumed to be negligible and the shift in x and y are estimated. Then, taking into account the estimated shift, the two scaling parameters are neglected and the rotation angle is estimated. Then, after applying the previous shift and rotation parameters, the two scaling parameters are computed. These scaling parameters are kept constant for the rest of the search.

(R3.2) The three previous rotation and shift parameters are iteratively refined, at better and better accuracies. For example, if the first step looks at an accuracy of 2 degrees rotation, and 2 pixels shift, four successive iterations will look at the respective accuracies of 1 degree/1 pixel , 0.5 degree/0.5 pixel, 0.25 degree/0.25 pixel.

The two differences between the edge-based registration and the wavelet-based registration reside in the type of features that are considered to perform the registration, edges versus wavelet coefficients, and in the size of the images on which the computations are carried out: for the edge-based registration, the full size images are utilized for every step. For the wavelet-based registration, the initial search is carried out on the lowest level of wavelet decomposition, i.e., the smallest size images, then each refinement is computed on the next size-up, with the final refinement being computed on the full size image. This last variation explains the difference in the number of operations needed for each algorithm, about 480 floating point operations per pixel for the edge-based registration versus about 200 floating point operations per pixel for the wavelet-based registration.

3. Results

These two algorithms have been tested with four different types of datasets:

- the first dataset represents *synthetic test patterns* where patterns and transformations are well-controlled.
- the second dataset is representative of *multi-temporal studies* and is formed with a series of AVHRR/LAC scenes over South Africa. For this application, a map of the coastlines is available so the images can be geo-registered to the map.
- the third dataset is an example of *landmark navigation* with a series of five GOES images of a landmark, "Cape Cod," which are registered to a reference image (or "chip") of this landmark.
- the fourth dataset represent examples of *channel-to-channel co-registration (or calibration)* with two series of five-channels GOES images for which channel-to-channel registration is performed.

3.1. Test Data

Figure 2 represents seven different test patterns which have been utilized to test the edge-based registration method. This series of test patterns was created to test the response of our edge-based algorithm to edge directions, local intensity variations as well as texture variations.

A few preliminary experiments were conducted by applying two known transformations to the original image data (in this case, a composition of a rotation and a translation), and then registering the transformed images to the original image using the edge-based automatic registration. Results are shown in Table 3 and indicate average absolute errors of 0.12 degree in rotation and 0.28 pixel in translation. Although these first results are very encouraging, the present size of the dataset is not sufficient to give any conclusions about the accuracy or the precision of the system, but it will be extensively tested in future experiments.

TEST PATTERN	"TRUE" TRANSFORM (Rot: degrees TranslX: pixels TranslY: pixels)			COMPUTED TRANSFORM			ERROR=|true-computed|		
	(Rot	TX	TY)	(Rot	TX	TY)	(Rot	TX	TY)
GRID2.2.15.15	(0.5	1.8	0.5)	(0.5	2.2	0.85)	(0	0.4	0.35)
	(1	0.5	1.5)	(1	0.95	1.9)	(0	0.45	0.4)
GRIDG2.2.15.15	(0.5	1.8	0.5)	(0.5	1.85	0.5)	(0	0.05	0)
	(1	0.5	1.5)	(0.7	0.6	0.75)	(0.3	0.1	0.75)
GRID5.5.20.20	(0.5	1.8	0.5)	(0.5	0.75	0.55)	(0	1.05	0.05)
	(1	0.5	1.5)	(1	0.6	1.55)	(0	0.1	0.05)
GRIDG5.5.20.20	(0.5	1.8	0.5)	(0.5	2.2	0.45)	(0	0.4	0.05)
	(1	0.5	1.5)	(0.75	0.55	0.75)	(0.25	0.05	0.75)
RING10.15	(0	0.8	0.2)	(0.15	0.65	0.25)	(0.15	0.15	0.05)
	(0	2	1)	(-0.25	1.75	1.5)	(0.25	0.25	0.5)
RING2.20	(0	0.8	0.2)	(0.3	0.6	0.2)	(0.3	0.2	0)
	(0	2	1)	(-0.45	0.75	1.35)	(0.45	1.25	0.35)
MOSAIC	(0.6	1.5	0.8)	(0.6	1.55	0.8)	(0	0.05	0)
	(1	0.6	1.5)	(1	0.65	1.5)	(0	0.05	0)
	Average Error Rotation: 0.12 Degrees								
	Average Error Translation: 0.28 Pixels								

Table 3

Results of the Automatic Edge-based Registration on the Test Pattern of Figure 2

3.2. AVHRR Data (Image to Map)

The second dataset is a series of 13 512 rows by 1024 columns AVHRR/LAC images over South Africa. Raw AVHRR data are navigated and georeferenced to a geographic grid that extends from -30.20 S, 15.39 E (upper left) -34.79 S, 24.59 E (lower right). The navigation process uses an orbital model developed at the University of Colorado [15] and assumes a mean attitude behavior (roll, pitch and yaw) derived using Ground Control Points [16]. A map of the coastline derived from the Digital Chart of the World (DCW) is generated for the same geographic grid. Figure 3 shows one image of this sequence superimposed with the map of the coastline. Note that in this case, there is a slight misregistration. The coastline map is used to create a mask, i.e. the area of the input images where the edge features are correlated with the map. Figure 4 shows these features in a [-20,+20] pixel interval around the coastline. After correlation, the {rotation,shift,scaling} transformation is computed and used to correct the input image. Figure 5 shows the corrected image superimposed with the map and Table 4 shows the registration results using the edge-based method.

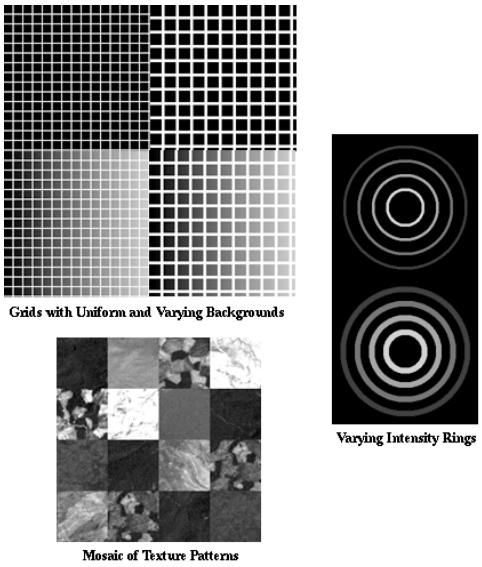

Figure 2
Test Patterns Including Grids, Rings, and a Texture Mosaic

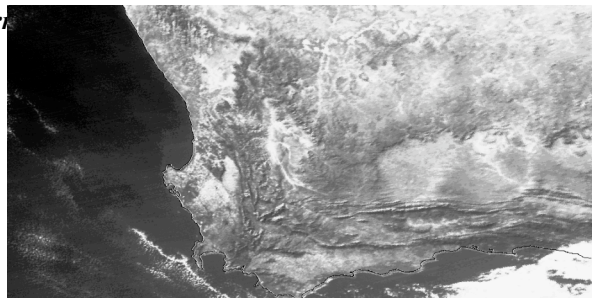

Figure 3
Original AVHRR South Africa Image with Coastline Map

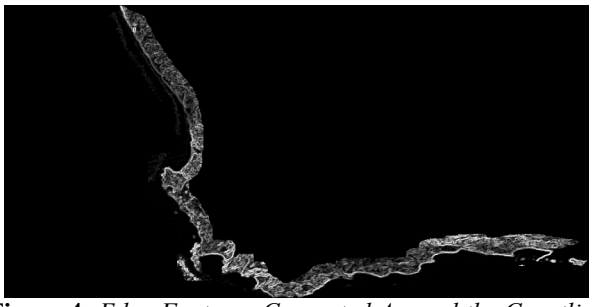

Figure 4 -*Edge Features Computed Around the Coastline*

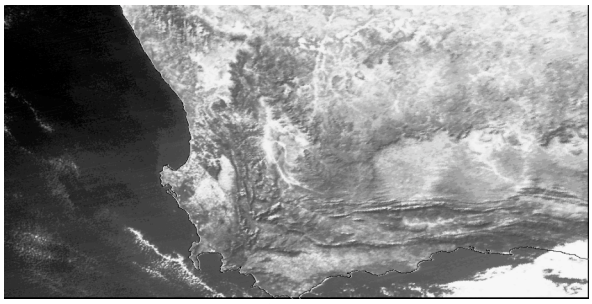

Figure 5
Corrected AVHRR South Africa Image with Coastline Map (Rotation=0 degrees, Shift=(2,3) pixels, Scalings =1)

DATA	sa125	sa126	sa127	sa129	sa1300	sa1311	sa1322	sa133	sa1411	sa143	sa146	sa1488
Iter. Edge Match												
Register to Map	(0,0)	(-1,-1)	(-1,-1)	(-1,-1)	(1,1)	(1,0)	(1,-1)	(0,-1)	(0,-1)	(-1,-3)	(-2,-2)	(2,3)

Table 4
AVHRR Data Registration Results (Edge-Based Method) (All Rotations=0, All Shifts=1, Only Shifts are Indicated)

3.3. GOES Data

3.3.1. Landmarking (Image to Landmark)

Landmark registration has usually two purposes: geo-registering new incoming images, as well as refining the satellite orbit computation and navigation system. Two recent studies dealing with satellite meteorological data show significant contribution in this domain. The first study [3] deals with Meteosat data, while the second one [4] concentrates on GOES data. Both studies consider a shift-only transformation, and obtain sub-pixel accuracy by up-sampling the data. The Meteosat study uses Normalized Cross-Correlation (NCC) on edges of landmarks such as coastlines. The GOES study uses only lakes and islands for landmarks, and evaluates six different matching methods. Among

these methods Cross-Correlation (CC) and NCC of enhanced gray levels, as well as Edge Matching are evaluated as performing the best; Edge Matching is the least sensitive to cloud cover, while (N)CC provides a slightly more accurate position estimation. Both studies also utilize a masking of the clouds in order to increase the reliability of the registration. The GOES study also provides a good procedure description and some requirements for the choice of the landmarks.

Our first landmarking tests using our wavelet-based algorithm were performed on a sequence of five successive 128x128 images from the GOES satellite over the Cape Cod area, "RAW1" to "RAW5", shown in Figure 6. Since we do not currently have a map database available which would be used to perform the landmark registration, we simulated this process by taking as reference "chip" a sub-image extracted from the center of the first image "RAW1". This reference chip is then automatically registered to the other images utilizing the wavelet-based registration algorithm described above.

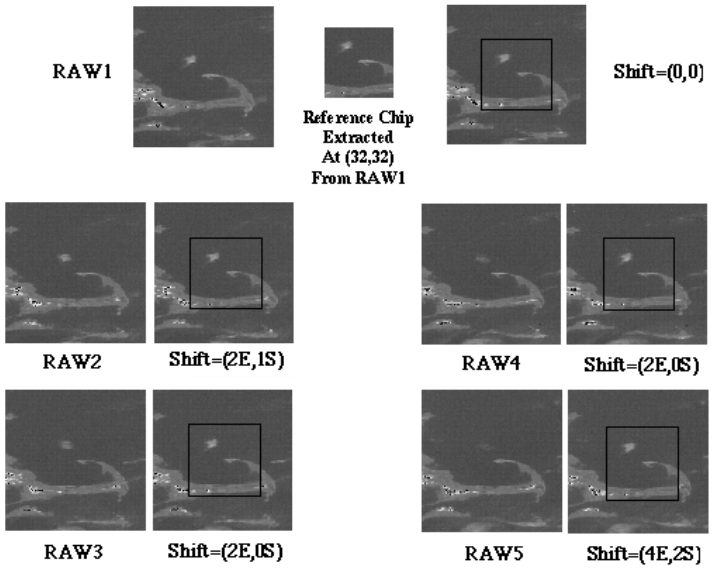

Figure 6
Wavelet-based Registration of a Sequence of Five GOES Images of Cape Cod.

As expected, when the reference chip is registered to the image from which it was extracted, the transformation which is computed is (0E,0S), which means that there is no shift towards the East or South directions. Then, the respective shifts between reference chip and input images are given for each of the input images "RAW2" to "RAW5", and the results are displayed in Figure 1 by a black window located at the shifted position which has been automatically computed by the algorithm. Qualitatively, these results look very satisfactory, and we can notice that even the presence of a small cloud in the reference chip which then disappears in the following images of the sequence does not seem to affect the results. Future work will include the use of a cloud masking as well as determining the maximum percentage of the image which can be covered by clouds without affecting the reliability of the algorithm [14].

3.3.2. Channel-to-Channel Co-Registration (Image-to-Image)

Channel-to-channel co-registration is a calibration-type operation which might not be necessary to perform for every image received by a multispectral instrument. Co-registration might be necessary when an instrument has just been launched, and then will be computed about twice a day (or even less often): at each of these computations a look-up-table will be updated with the five co-registration parameters (rotation, shift, and scaling). Depending on the number of channels, instead of computing these parameters on every possible pair of channels, a reference channel from each focal plane (or each group of channels) can be selected and co-registration is computed in two steps:
Step 1: reference channels are co-registered to the highest-resolution channel which is visible at that time of the day,
Step 2: every channel of a given group is co-registered to the reference channel of this group.
For example, for the 5 GOES channels, Channels 1 (Visible) and 4 (Long Wave-IR) are taken as reference channels. So the co-registration is performed on the following cascade of pairs of channels:
Step 1: (1,4)
Step 2: (4,2), (4,3), (4,5)

To our knowledge, no systematic study has been attained for the co-registration of remote sensing data, in particular meteorological satellite data. In this case, the issues are somewhat different from the general image registration problem:
• The transformations to be considered are in general smaller. For example, we can assume that:
  •• rotations will vary in the interval [-1°,+1°],
  •• translation shifts in [-2pixels,+2pixels],
  •• scaling factors in [-0.9pixels,+0.9pixels].
• Although the observed areas are about the same in each channel, the visible features can be quite different, which leads to two main differences with the general image registration problem:
  •• coastline registration is not always applicable,
  •• clouds should be used and not eliminated from the registration process.
• The highest-resolution channel which is utilized as a reference will be different for different times of the day and its spatial resolution will be lower at night.

This set of experiments was performed utilizing multiple channels of a sequence of GOES images taken during 24 hours in two different sectors, "Baja" and "Florida". There are 5 GOES channels with the respective spatial resolutions of 1 km and 4 km. Figure

7a shows the 5 channels of a GOES scene of the "Baja" sector. After basic preprocessing of the data and in order to deal with similar spatial resolution data, a wavelet decomposition of Channel 1 is performed (see Figure 7b). After 2 decomposition levels, the spatial resolution of the decomposed Channel 1 is identical to the resolution of Channels 2 to 5. Then a Sobel edge detection is computed on the compressed Channel 1 and on Channels 2 to 5 (see Figure 7c), and the edge-based registration described above is applied to these edge features. We can notice that Channel 3 (Water Vapor Channel) does not present the same original or edge features as the other channels and this remark explains the following results relative to the registration of Channel 3.

We tested 33 five-channel scenes corresponding to the "Baja" sector. According to the two steps described earlier, we chose Channel 1 as the reference channel for the visible wavelength, and Channel 4 as the reference channel for the infra-red wavelength; then the cascade of channels to register is: (1,4), (4,2), (4,3), (4,5). For each of the 33 scenes, three tests of registration were performed:

(E1) All original channels are registered

(E2) Channel 1 was artificially translated by the vector (1,2) pixels, leaving Channels 2 to 5 unchanged,

(E3) Channel 1 was artificially rotated by the angle 0.5 degrees and translated by the vector (0.5,1.2) pixels, while Channels 2 to 5 were unchanged.

Table 5 shows some results of these experiments, detailed for the first three scenes, and then the accuracy and the standard deviation (or precision) of the rotation and translation parameters is computed over the 33 scenes for the four pairs of channels. The accuracy and the standard deviation of a parameter "a" are computed according to the following formulas:

$$\text{Accuracy (a)} = \frac{1}{33*3} \sum_{i=1}^{i=33*3} (a(i) - \text{true\_a})$$

and

$$\text{StdDev (a)} = \frac{1}{33*3} \sum_{i=1}^{i=33*3} ((a(i) - \text{true\_a})^2) - (\text{Accuracy(a)}^2)$$

Correlation coefficients, which vary between 0 and 1, are also indicated for each registration. The results show a perfect registration of Channels 4 and 5 with a correlation coefficient close to 1, and a relatively good registration of Channels 4 and 2. As we noticed previously, the features extracted from Channel 3 do not permit a good registration and it is illustrated by very low correlation coefficients (around or below 0.1). In this example, the registration of Channels 1 and 4 seems to present a bias of (0.95,0) in shift that is consistent among the 33 scenes of this sequence. In the absence of ground truth data and with correlation coefficients of average value, no conclusion could be drawn from this result. If additional information was available, such registration could indicate a shift in the geometric calibration of Channel 1 relative to the other channels.

Image	Channels 1/4			Channels 4/2			Channels 4/3			Channels 4/5		
	Rot. (Deg.)	Transl. (Pix.)	Correl	Rot. (Deg.)	Transl. (Pix.)	Correl	Rot. (Deg.)	Transl. (Pix.)	Correl	Rot. (Deg.)	Transl. (Pix.)	Corr.
...101615...												
Original	0.15	0.95,0.35	0.44	0	0.2,0.2	0.65	0.15	-0.85,-0.1	0.12	0	0,0	0.94
R=0 T=(1,2)	0.1	1.9,2.3	0.44	-	-	-	-	-	-	-	-	-
R=.5 T=(.5,1.2)	0.5	1.55,1.25	0.44	-	-	-	-	-	-	-	-	-
...101632...												
Original	0.15	0.85,0.1	0.44	0	0,0	0.64	0.35	-1.6,0.65	0.05	0	0,0	0.94
R=0 T=(1,2)	0.05	1.95,2.05	0.44	-	-	-	-	-	-	-	-	-
R=.5 T=(.5,1.2)	0.5	1.55,1.25	0.44	-	-	-	-	-	-	-	-	-
...101645...												
Original	0	1,0	0.44	0	0,0	0.65	0.15	-1.1,0.15	0.11	0	0,0	0.94
R=0 T=(1,2)	0	2,2	0.44	-	-	-	-	-	-	-	-	-
R=.5 T=(.5,1.2)	0.5	1.55,1.25	0.44	-	-	-	-	-	-	-	-	-
After 33 Experiments:												
Accuracy	**-0.06**	**(-0.72,-0.18)**		**0**	**(0.01,0.01)**		**-0.217**	**(0.62,-0.19)**		**0**	**(0,0)**	
Stand. Dev.	**0.07**	**(0.29,0.13)**		**0**	**(0.04,0.04)**		**0.115**	**(0.85,0.32)**		**0**	**(0,0)**	

Table 5
Results of Registration Experiments for the "Baja" Sector, Fig.7a

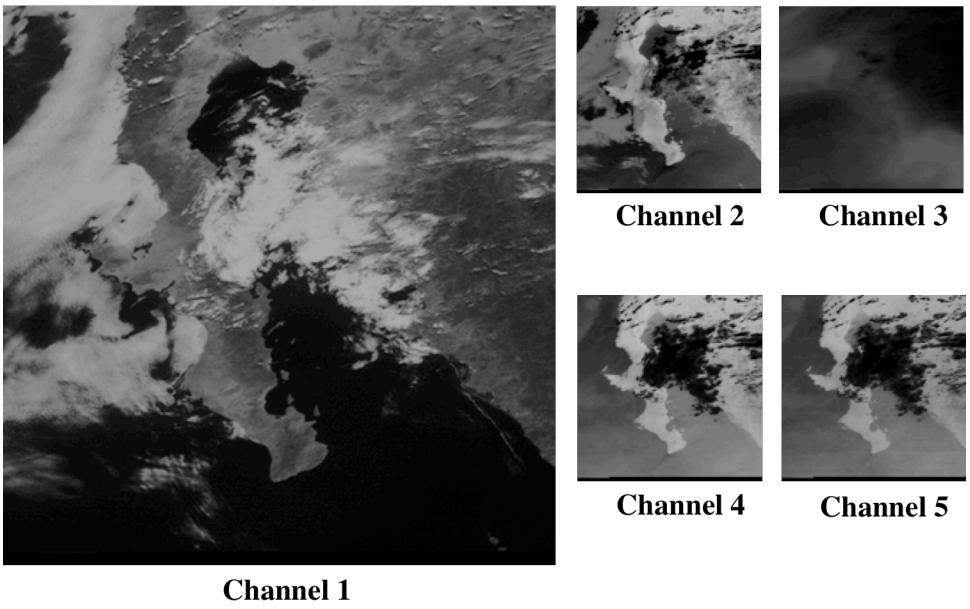

Figure 7a
GOES Scene; "Baja" Sector; Five Channels
(Images reduced for display purposes)

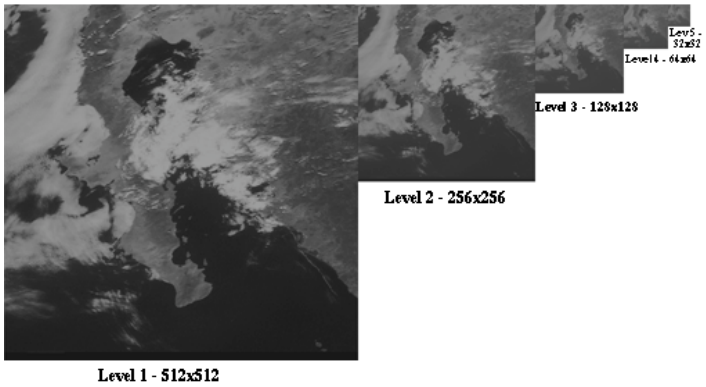

Figure 7b - ***Wavelet Decomposition of Channel 1 shown in Figure 7a***

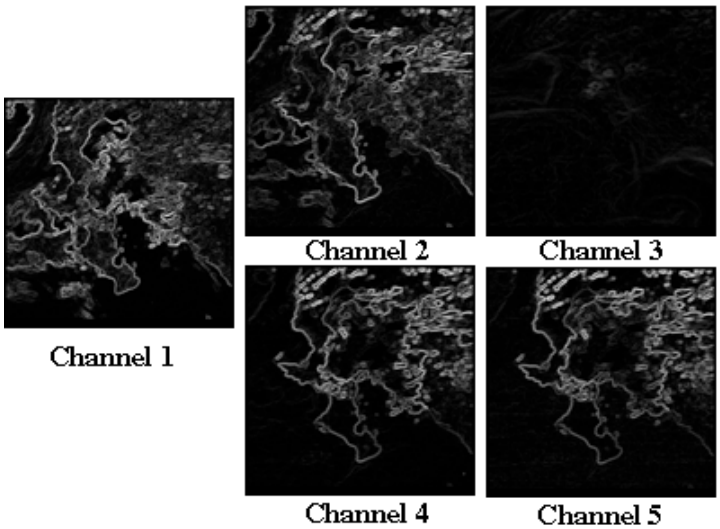

Figure 7c - ***Edge Detection on Level2-Wavelet of Channel 1 and on Channels 2 to 5 of Figure 7a***

Similar experiments were conducted with the successive scenes of the "Florida" sector shown in Figure 8a. In this case, no land features are visible in any of the five channels and this example shows how channel-to-channel co-registration can be performed with only cloud features. Figure 8b shows the edges extracted from the five channels and Table 6 details the results of the registrations performed for the above experiments (E1), (E2) and (E3). These few results show good registrations of the five channels

4. Conclusion and Future Work

These preliminary experiments utilizing edge- and wavelet-based image registration are very promising. Still more work needs to be done in the following areas:

- *Sub-pixel accuracy:* from the previous GOES and Meteosat studies, we feel that automatic registration schemes based on edge or edge-like features should be able to achieve sub-pixel accuracy. Of course a landmark registration at such an accuracy assumes that a map database will be available at a very high resolution (e.g., DMA map) and for a very large number of landmarks. If needed, accuracy can also be improved by interpolating the correlation curve using for example a cubic-spline method.
- *Robustness of Algorithms:* The robustness of the algorithm will have to be evaluated in function of variable conditions (such as time of day), especially for the co-registration process, since different channels with a lower spatial resolution will have to be utilized as reference at night. Robustness will also have to be evaluated relative to the issue of cloud occlusion.
- *Dependency on Initial Conditions:* The cost of computing the spatial correlation of two images is a function of the number of steps where the correlation is computed. If we perform the correlation of 2 images of size NxM at k different positions, the computational cost is equal to 2*k*N*M floating point operations. So if the initial search for the five parameters is computed in some interval [-n,+n] with a step of 1, the correlation cost is: 2NM*(2*(2n+1)**2+(2n+1)). If the initial search interval increases, i.e., the accuracy of the initial parameters given by the attitude model decreases, then the computational cost of the registration will increase according to the above formula. A larger uncertainty in the initial conditions might also lead to false paths in the search for registration parameters and therefore decrease the overall registration accuracy.

In general, quantitative testing, as well as accuracy and simulation studies will be pursued for the two previous types of registration for the purpose of multi-temporal registration, landmark navigation, as well as channel-to-channel co-registration.

Acknowledgments
The authors would like to thank Bill Campbell and the NASA/ Goddard Space Flight Center's Applied Information Sciences Branch for their support in the development of the algorithms, as well as Jim Tucker, Dennis Chesters, Del Jenstrom, Sanford Hinkal, Rick Lyon, and the GATES project team for providing advise, expertise and data for our experiments.

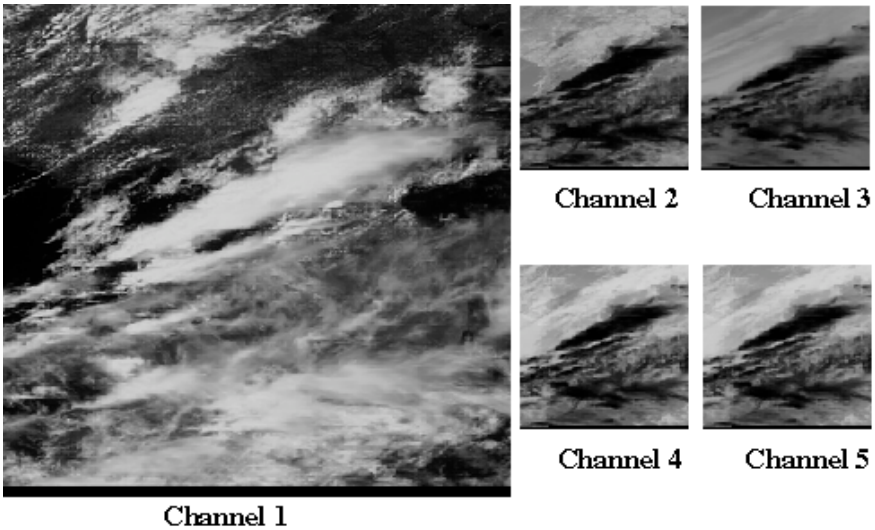

Figure 8a - ***GOES Scene; "Florida" Sector; Five Channels (Images reduced for display purposes)***

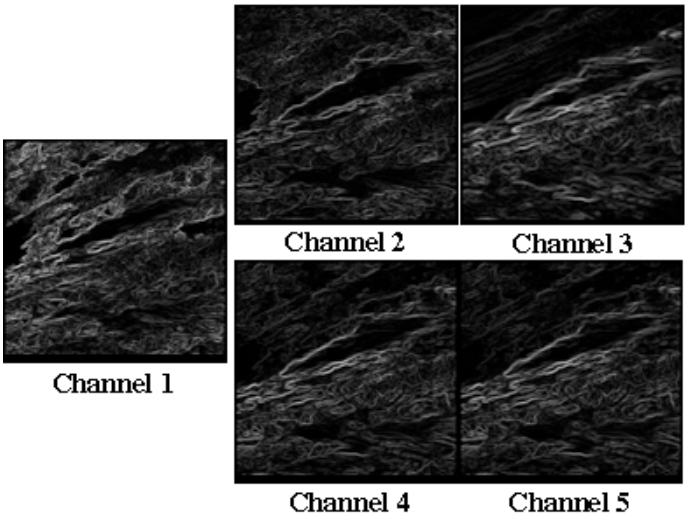

Figure 8b - ***Edge Detection on Level2-Wavelet of Channel 1 and on Channels 2 to 5 of Figure 8a***

Image	Channels 1/4			Channels 4/2			Channels 4/3			Channels 4/5		
	Rot.	Transl.	Corr.	Rot.	Transl.	Corr.	Rot.	Transl.	Corr.	Rot.	Transl.	Corr.
	(Deg.)	(Pix.)		(Deg.)	(Pix.)		(Deg.)	(Pix.)		(Deg.)	(Pix.)	
Original	0	(0,0)	0.47	0	(-.4,-.4)	0.68	0	(0,0)	0.72	0	(0,0)	0.98
R=0 T=(1,2)	0	(1,2)	0.47	-	-	-	-	-	-	-	-	-

Table 6 - ***Results of Co-registration Experiments for the Scene of the "Florida" Sector (Fig.8a)***

Bibliography

[1] L.Brown, "A Survey of Image Registration Techniques," *ACM Comp.Surv.,* Vol 24, 4, 1992.

[2] J. Le Moigne et al, "An Automated Parallel Image Registration Technique of Multiple Source Remote Sensing Data," CESDIS TR-96-182 - submitted to *IEEE Trans.Geosc. and Rem. Sens.*

[3] B. Blancke, J.L. Carr, E. Lairy, F. Pomport, B. Pourcelot, "The Aerospatiale Meteosat Image Processing System (AMIPS)," *1-st Intern. Symp. Scientific Imagery & Im. Proc*., Cannes, France, Apr. 1995.

[4] W. Eppler, D. Paglieroni, M. Louie, J. Hanson, "GOES Landmark Positioning System," SPIE Proceedings Vol. 2812, Intern. Symp. on OPtical Science, Engin., and Instrumentation, GOES-8 and Beyond, Denver, CO, August 4-9, 1996.

[5] J.C. Tilton, "Comparison of Registration Techniques for GOES Visible Imagery Data," *IRW97*, NASA-GSFC, Oct. 97.

[6] W.K. Pratt, "Correlation Techniques of Image Registration," *IEEE Trans. Aerosp. and Electr. Systems,* Vol.AES-10, 3, 1974.

[7] J. Canny, "Computational Approach to Edge Detection," IEEE-PAMI, Vol.8, Nov. 1986.

[8] J. Shen, S. Castan, "An optimal linear operator for step edge detection," *Graphical Models and Image Processing*, Vol. 54, No. 2, 1992.

[9] R.F. Cromp, W. J. Campbell, "Data Mining of Multidimensional Remotely Sensed Images," *Proc. 2nd Int. Conf. on Information and Knowledge Management*, Wash.DC, Nov. 1993.

[10] J.LeMoigne,"Parallel Registration of Multisensor Remotely Sensed Images Using Wavelet Coefficients," *SPIE Aerosense,* Apr. 1994.

[11] J. Le Moigne, "Towards a Parallel Registration of Multiple Resolution Remote Sensing Data," *IGARSS'95,* Firenze, Italy, July 1995.

[12] D.I. Barnea, and H.F. Silverman, "A Class of Algorithms for Fast Digital Registration," *IEEE Trans. on Computers*, Vol. C-21, 179-186, 1972.

[13] D. Mount, N. Netanyahu, J. LeMoigne, "An Efficient Algorithm for Robust Feature Matching", *IRW97,* NASA-GSFC, Oct. 97.

[14] M. McGuire, H. Stone, "Techniques for Multi-Resolution Image Registration in the Presence of Occlusions," *IRW97*, NASA-GSFC, Oct. 97.

[15] G.W. Rosborough, D.G. Baldwin, W.J. Emery, "Precise AVHRR Image Navigation," *IEEE Transactions on Geoscience and Remote Sensing*, Vol. 32, No. 3, May 1994.

[16] D. Baldwin, W. Emery, "Spacecraft Attitude Variations of NOAA-11 Inferred from AVHRR Imagery," Int. J. of Remote Sensing, Vol. 16, No. 3, 531-548, 1995.